

# Molecular Dynamics Calculations of the Hard-Sphere Equation of State

Jerome J. Erpenbeck<sup>1</sup> and William W. Wood<sup>1,2</sup>

Received October 12, 1983; revisions received October 21, 1983 and December 6, 1983.

---

The equation of state of the hard-sphere fluid is studied by a Monte Carlo-molecular dynamics method for volumes ranging from  $25V_0$  to  $1.6V_0$ , where  $V_0$  is the close-packed volume, and for system sizes from 108 to 4000 particles. The  $N$  dependence of the equation of state is compared to the theoretical dependence given by Salsburg for the  $NPT$  ensemble, after correction for the ensemble difference, in order to obtain estimates for the thermodynamic limit. The observed values of the pressure are compared with both the [3/2] and the [2/3] Padé approximants to the virial series, using Kratky's value for the fifth virial coefficient  $B_5$  and choosing  $B_6$  and  $B_7$  to obtain a least-squares fit. The resulting values of  $B_6$  and  $B_7$  lie within the uncertainties of the Ree-Hoover-Kratky Monte Carlo estimates for these virial coefficients. The values of  $B_8$ ,  $B_9$ , and  $B_{10}$  predicted by our optimal [3/2] approximant are also reported. Finally, the Monte Carlo-molecular dynamics equation of state is compared with a number of analytic expressions for the hard-sphere equation of state.

---

**KEY WORDS:** Equation of state; hard spheres, virial series; Monte Carlo; molecular dynamics; Padé approximants;  $N$  dependence.

## 1. INTRODUCTION

The equation of state of the hard-sphere fluid has been obtained by numerical statistical mechanics methods by a number of authors, beginning with the pioneering Monte Carlo calculations of Metropolis *et al.*<sup>(1)</sup> for

---

Work supported by the Office of Basic Energy Sciences, U.S. Department of Energy.

<sup>1</sup> Los Alamos National Laboratory, Los Alamos, New Mexico 87545.

<sup>2</sup> Present address: Carroll College, Helena, Montana 59601.

systems of  $N = 256$  particles and Wood and Jacobson<sup>(2)</sup> for  $N = 32$ , as well as the molecular dynamics calculations of Alder and Wainwright<sup>(3)</sup> for  $N = 32$  and 108. These early results have been reviewed by Wood.<sup>(4)</sup> More extensive Monte Carlo calculations have been reported by Barker and Henderson<sup>(5)</sup> (for  $N = 108$ ), who also report results for the pair-correlation function.

With the advent of perturbation theories for fluids (for a review see Ref. 6) the importance of detailed and precise results for hard spheres is increased by virtue of the role of the hard-sphere system as the reference system in most such theories. In addition, the hard-sphere equation of state continues to occupy a pivotal role in the development of both approximate and exact equation-of-state theories. Of particular importance in this regard are developments based upon the virial series, especially those using the Padé<sup>(7,8)</sup> and other<sup>(9)</sup> approximant techniques in attempts to extend the virial series into the dense-fluid and even the unstable-fluid regimes. These developments have led to considerable controversy (for a review see Ref. 10) with regard to the nature of the singularities of the virial series.

The numerical methods of Monte Carlo (MC) and molecular dynamics (MD) which are used to obtain the equation of state yield results only for small finite systems. A central problem concerns the extrapolation to the thermodynamic limit. In a study of the equation of state of hard disks, Wood<sup>(11)</sup> showed that systems as large as 48 particles at high fluid densities exhibited an anomalous dependence of the pressure on  $N$ , so that larger systems needed to be studied in order to estimate the thermodynamic limit accurately. It is our purpose here to study the hard-sphere equation of state in similar detail.

Our results for the equation of state differ from previous estimates in two respects. First, they are statistically more precise because of the extreme length of many of our calculations,<sup>3</sup> having statistical uncertainties at least an order of magnitude smaller than earlier results. Secondly, our values of the pressure take into account the correct dependence on system size, both theoretically and through the evaluation of the pressure for much larger system sizes than previously investigated.

We compare our estimates of the equation of state with the predictions of the virial series, using for the latter several Padé approximants which depend on virial coefficients up to  $B_7$ . The values of  $B_1$  through  $B_4$  are known exactly, and  $B_5$  has been accurately estimated by Kratky<sup>(8)</sup> using Monte Carlo evaluation of the Mayer and Mayer–Montroll graphs, improving on the accuracy of the earlier estimates by Ree and Hoover.<sup>(7)</sup> The

<sup>3</sup> These long calculations are carried out in connection with the estimation of the super-Burnett coefficient<sup>(12)</sup> and the time-correlation function for shear viscosity.<sup>(13)</sup>

coefficients  $B_6$  and  $B_7$  were estimated by Ree and Hoover<sup>(7)</sup> by Monte Carlo evaluation of the modified Mayer graphs (Ree–Hoover graphs). Kratky<sup>(8)</sup> has recently reassessed the accuracy of these estimates. We find small but significant discrepancies between our numerical results and the equation of state as estimated by the Padé approximants which are available from knowledge of these virial coefficients when we use the “best” values given by Kratky. However, by adjusting  $B_6$  and  $B_7$  for optimal agreement of these approximants with our results, we obtain satisfactory statistical concordance as well as values of  $B_6$  and  $B_7$  which lie within Kratky’s estimates of the error bounds. In addition, reexpansion of our optimal approximant into a virial series gives values of  $B_8$  through  $B_{10}$  which are similar to various estimates given by Kratky.

In Section 2 we describe our numerical method, and in Section 3 we discuss our results for finite systems. The extrapolation to the thermodynamic limit and the related fitting of our results to the virial series are presented in Section 4. In Section 5 we compare our equation of state to various analytic results.

## 2. METHOD

We consider a system of  $N$  classical particles, each of mass  $m$  in volume  $V$ , subject to periodic boundary conditions.<sup>(4)</sup> If we denote the positions and velocities of the particles by  $\mathbf{x}^N = (\mathbf{r}^N, \mathbf{v}^N)$  in which  $\mathbf{r}^N = (\mathbf{r}_1, \mathbf{r}_2, \dots, \mathbf{r}_N)$  and  $\mathbf{v}^N = (\mathbf{v}_1, \mathbf{v}_2, \dots, \mathbf{v}_N)$ , then it has been shown<sup>(14)</sup> that the dynamical pressure  $p_{\text{MD}}$  is given through the compressibility factor,

$$Z_{\text{MD}} = \frac{p_{\text{MD}}V}{Nk_B T_{\text{MD}}} = 1 - \frac{\bar{W}}{\bar{K}} \quad (1)$$

where  $k_B$  is the Boltzmann constant, and  $\bar{F}$  denotes the long-time average of a phase function  $F(\mathbf{x}^N)$ .

$$\begin{aligned} \bar{F} &= \lim_{t \rightarrow \infty} \bar{F}(t) \\ \bar{F}(t) &= \frac{1}{t} \int_0^t dt' F[\mathbf{x}^N(t')] \end{aligned} \quad (2)$$

In writing the phase  $\mathbf{x}^N(t)$  as a function of the time, we shall follow the “infinite checkerboard”<sup>(14)</sup> definition whereby  $\mathbf{r}_i(t)$  is the integral of the velocity and thus will not necessarily lie in the primary cell other than at  $t = 0$ . In addition,  $\bar{K}$  is the kinetic energy in the center-of-mass frame of

reference,

$$\begin{aligned}\hat{K}(\mathbf{v}^N) &= K(\mathbf{v}^N) - M^2/2mN \\ K(\mathbf{v}^N) &= (m/2) \sum_{i=1}^N v_i^2 \\ \mathbf{M}(\mathbf{v}^N) &= m \sum_{i=1}^N \mathbf{v}_i\end{aligned}\quad (3)$$

$W(\mathbf{r}^N)$  is the virial function, which for pair interactions  $u(\mathbf{r})$  and periodic boundary conditions is

$$\begin{aligned}W(\mathbf{r}^N) &= -\frac{1}{2} \sum_{\nu} \sum'_{j < i} (\mathbf{r}_{ij} + \nu L) \cdot \mathbf{F}(\mathbf{r}_{ij} + \nu L) \\ \mathbf{r}_{ij} &= \mathbf{r}_i - \mathbf{r}_j \\ F(\mathbf{r}) &= -\frac{du(\mathbf{r})}{d\mathbf{r}}\end{aligned}\quad (4)$$

and  $T_{\text{MD}}$  denotes the molecular dynamics temperature,

$$T_{\text{MD}} = 2\bar{K}/3k_B N \quad (5)$$

Finally,  $\mathbf{M}$  is the total linear momentum and  $L = V^{1/3}$  denotes the length of the periodic cell which we have taken to be cubic in all the numerical calculations. Thus the  $\nu$  sum in Eq. (4), defined as the sum over triples of signed integers,

$$\sum_{\nu} = \sum_{\nu_1} \sum_{\nu_2} \sum_{\nu_3}$$

includes interactions between each particle  $i$  and both  $j$  and the various images of  $j$ . The prime on the  $i, j$  sum denotes that the "self-term"  $i = j$  is omitted for  $\nu = 0$ .

For the impulsive hard-sphere interaction, the kinetic energy is equal to the total energy  $E(\mathbf{v}^N)$  and both the total energy and the energy in the center-of-mass frame of reference,

$$\hat{E} = E - M^2/2mN \quad (6)$$

are constants of the motion, because of the conservation of linear momentum in the absence of external forces. Moreover, the time-averaged virial reduces to a sum over collisions,

$$\bar{W}(t) = -\frac{m}{2t} \sum_{\gamma=1}^{c(t)} \boldsymbol{\sigma}_{ij}(t_{\gamma}) \cdot \Delta \mathbf{v}_i(t_{\gamma}) \quad (7)$$

where  $c(t)$  is the number of collisions up to time  $t$ ,  $\boldsymbol{\sigma}_{ij}$  is the line-of-centers vector for the colliding pair  $i = i(\gamma)$  and  $j = j(\gamma)$  (with  $|\boldsymbol{\sigma}_{ij}| = \sigma$ , the hard-

sphere diameter), and  $\Delta v_i(t_\gamma)$  the change in velocity of particle  $i$  on the  $\gamma$ th collision.

The relation of the dynamical pressure to that for the canonical ( $NVT$ ) ensemble is, for hard spheres,<sup>(14)</sup>

$$Z_{NVT} - 1 = \frac{N-1}{N} (Z_{MD} - 1) \quad (8)$$

$$Z_{NVT} = \frac{p_{NVT}V}{Nk_B T}$$

In the next section, we report values for  $Z_{NVT}$  for the  $NVT$  ensemble.

Our dynamical calculations consist not of a single trajectory as is common in molecular dynamics; instead a number of trajectories are generated, with the initial phase  $\mathbf{x}^N(0)$  sampled via the ordinary Metropolis Monte Carlo method<sup>(4)</sup> from either the microcanonical ( $NVE$ ) ensemble or the molecular dynamics ( $NVEM$ ) ensemble. Our use of a combination of Monte Carlo and molecular dynamics (MCMD) permits a number of ways of computing the pressure and we present results for the methods which appear to yield the smallest statistical uncertainty. In particular, we form the Monte Carlo average of the quantity  $\overline{W}(t_f)/\hat{E}$  in which  $t_f$  denotes the final time to which each trajectory is generated. We proceed by relating this to the  $NVT$  ensemble pressure.

For this purpose, we compute the expectation value of this quantity in the  $NVE$  ensemble. Using Liouville's theorem, we readily show that  $\langle \overline{W}(t)/\hat{E} \rangle_{NVE}$  is independent of  $t$ . Then using  $\overline{W}$  from Eq. (7), we find for  $t$  sufficiently small that the first collision need only be taken into account,

$$\langle \overline{W}(t)/\hat{E} \rangle_{NVE} = - \frac{m}{4N(N-1)t} \langle \sigma_{12} \cdot \mathbf{v}_{12} A(t - t_1^{(12)})/\hat{E} \rangle_{NVE} \quad (9)$$

where  $t_1^{(12)}$  denotes the time of the first collision between particles 1 and 2 and where  $A(x)$  is the unit-step function. By introducing relative coordinates  $\mathbf{r}_{12}$  and introducing the pair-correlation  $g_{NV}(r_{12})$  by integrating over the coordinates of particles 2, 3, . . . ,  $N$ , we obtain

$$\langle \overline{W}(t)/\hat{E} \rangle_{NVE} = - \frac{1}{6} mn^2 \sigma^3 V g_{NV}(\sigma) \langle v_{12}^2/\hat{E} \rangle_{NVE} \quad (10)$$

The average  $\langle v_{12}^2/\hat{E} \rangle_{NVE}$  can be evaluated explicitly by following the methods given in Ref. 14; we obtain

$$m \langle v_{12}^2/\hat{E} \rangle_{NVE} = 4/(N-1) \quad (11)$$

Substituting into Eq. (10) and introducing the pressure in the  $NVE$  ensemble through its well-known relationship to the pair-correlation function at contact,<sup>(4)</sup> we obtain

$$Z_{NVT} = 1 - \left(1 - \frac{1}{N}\right) \langle \overline{W}(t)/\hat{E} \rangle_{NVE} \quad (12)$$

Thus our Monte Carlo–molecular dynamics estimates for  $\langle \bar{W}(t)/\hat{E} \rangle_{NVE}$  yield estimates for the  $NVT$  ensemble equation of state.

For our calculations in the molecular dynamics ensemble ( $NVEM$ ), the expectation value of  $\bar{W}(t)/\hat{E}$  simplifies because  $\hat{E}$  is fixed (i.e., independent of trajectory). It is readily shown that  $\langle \bar{W}(t)/\hat{E} \rangle_{NVEM} = \langle \bar{W}(t) \rangle_{NVEM}/\hat{E}$ , independently of  $t$ , whence it reduces to  $\bar{W}/\hat{E}$ . Thus, by Eqs. (1) and (2),

$$Z_{NVT} = 1 - \left(1 - \frac{1}{N}\right) \frac{\langle \bar{W}(t) \rangle_{NVEM}}{\hat{E}} \quad (13)$$

Depending on the ensemble, then, we use either Eq. (12) or Eq. (13) to compute our estimates for the compressibility factor for the  $NVT$  ensemble. We refer to these estimates as the MCMD equation of state.

An additional method for computing the equation of state in a dynamical calculation is based on the collision rate,<sup>(14)</sup>

$$Z_{MD} = 1 + \frac{(2\sqrt{2})\pi\Lambda}{3\tau\alpha(N)\Lambda_0(\infty)} \quad \tau = V/V_0 \quad (14)$$

$$\alpha(N) = \frac{(3N/2)^{1/2}\Gamma[3(N-1)/2](1-1/N)}{\Gamma[(3(N-1)+1)/2]}$$

$$\approx 1 - 5/12N + O(N^{-2})$$

where  $V_0 = (\sqrt{2}/2)N\sigma^3$  is the close-packed volume,  $\Gamma(x)$  is the gamma function,  $\Lambda$  is the collision rate, and  $\Lambda_0(\infty)$  is the Boltzmann collision rate in the large-system limit,

$$\Lambda_0(\infty) = \frac{N}{2t_{00}}$$

$$t_{00} = \frac{1}{4\sigma^2 n} \left( \frac{m\beta_{MD}}{\pi} \right) \quad (15)$$

$$\beta_{MD} = 1/k_B T_{MD}$$

Note that  $t_{00}$  is the Boltzmann mean free time in the large-system limit. We have applied the collision-rate method only in the molecular dynamics ensemble.

### 3. RESULTS

Monte Carlo–molecular dynamics calculations of the equation of state have been made for ten values of the volume, relative to the close-packed volume  $V_0$ , shown in Table I, for as many as four different system sizes, ranging from  $N = 108$  to  $N = 4000$ . The values of  $Z_{NVT}$  obtained from the

Table I. Hard-Sphere Equation of State from Monte Carlo-Molecular Dynamics Calculations<sup>a</sup>

$\tau$	$N$	$\epsilon$	$N_{mc}$	$N_t$	$N_c$	$t_f/t_{00}^{(N)}$	$Z_{NVT}$		$\chi^2$
							from $W(\mathbf{r}^N)$	from $\Lambda$	
25	4000	1	30	50	17	160	1.12777 ± 0.00003		2.7
18	4000	1	30	73	26	160	1.18282 ± 0.00005		0.2
10	500	1	30	150	11	240	1.35881 ± 0.00011		0.1
	4000	1	30	98	38	60	1.35939 ± 0.00007		0.3
5	108	1	30	100	6	720	1.88374 ± 0.00050		1.1
	500	1	30	200	12	160	1.88729 ± 0.00027		
	500	1	30	100	6	160	1.88769 ± 0.00042		
							1.88742 ± 0.00023		0.1 <sup>b</sup>
	4000	1	30	50	24	160	1.88839 ± 0.00022		0.1
4	108	1	30	100	13	1440	2.23797 ± 0.00033		0.5
	1372	1	30	50	12	200	2.24356 ± 0.00036		0.5
3	108	2	200	100	45	4000	3.02250 ± 0.00032	3.02252 ± 0.00031	1.0
	500	2	200	105	108	2000	3.02964 ± 0.00022	3.02975 ± 0.00016	0.3
	1372	1	100	31	4	100	3.03225 ± 0.00095		1.8
	4000	1	50	99	65	160	3.03065 ± 0.00030		
	4000	2	50	100	74	180	3.03162 ± 0.00028	3.03146 ± 0.00022	
							3.03114 ± 0.00021		2.1 <sup>b</sup>
2	108	1	200	72	1	100	5.82774 ± 0.00486		
	500	1	200	32	3	100	5.85068 ± 0.00323		1.4
	1372	1	100	15	3	100	5.85641 ± 0.00380		0.4
	4000	1	30	50	52	160	5.85016 ± 0.00085		0.4
1.8	4000	1	50	50/42	63/53	160	7.43040 ± 0.00127		0.2 <sup>c</sup>
1.7	4000	1	100	88/82	49/46	64	8.60034 ± 0.00128		0.0 <sup>c</sup>
1.6	108	2	200	88	71	3000	10.08822 ± 0.00160	10.08813 ± 0.00154	
	500	2	200	72	72	800	10.19368 ± 0.00150	10.19286 ± 0.00149	
	500	2	200	16	16	800	10.19395 ± 0.00281		
							10.19373 ± 0.00132		2.5 <sup>b</sup>
	4000	1	100	100/90	64/58	64	10.19203 ± 0.00171		Foot-note c
	4000	2	500	100/97	79/77	80	10.19525 ± 0.00125	10.19810 ± 0.00131	Foot-note c
							10.19388 ± 0.00102		2.0 <sup>c</sup>

<sup>a</sup> $\epsilon$  denotes the ensemble, 1 for the  $NVE$  ensemble and 2 for  $NVEM$  ensemble,  $N_{mc}$  is the number of attempted Monte Carlo moves per particle between each of the initial configurations of the  $N_t$  trajectories.  $N_c$  is the total number of collisions over all trajectories, in millions.  $t_f$  is the final time on the MD trajectories in units of the Boltzmann mean free time  $t_{00}^{(N)}$ .

<sup>b</sup>Weighted mean of the preceding two values.

<sup>c</sup>Early trajectories were omitted to eliminate the effects of solidlike initial configurations. The actual number of trajectories and collisions which enter the reported values of  $Z_{NVT}$  are given after the solidus.

virial reported in Table I have been corrected to the  $NVT$  ensemble through either Eq. (12) or (13), depending on which ensemble was used. The length of each trajectory is listed in the table in units of the Boltzmann mean free time for the  $NVE$  ensemble,

$$t_{00}^{(N)} = \frac{N}{N-1} t_{00}$$

The Monte Carlo procedure used the so-called "cyclical" move prescription, in which each one of  $N - 1$  particles is given a trial displacement in cyclic order, beginning from the face-centered cubic (fcc) configuration. A number of attempted moves per particle,  $N_{mc}$ , was made in proceeding from the initial configuration for one trajectory to the initial configuration for the next trajectory. The initial velocities for each trajectory were selected from the appropriate distribution by an independent-trials method.<sup>4</sup> In choosing  $N_{mc}$ , it was intended that the values of the pressure would be essentially independent from trajectory to trajectory. Standard statistical procedures to test that hypothesis were used and found for the most part to be adequately satisfied. In several cases it was necessary to coarse-grain the results from two successive trajectories to satisfy these tests. At high density it was found that a number of the early trajectories appeared to yield low values for the pressure, indicating that an insufficient number of Monte Carlo moves had been taken to permit the fcc structure to melt. In these cases, the results for these early trajectories were omitted from the calculation of the reported pressure.

For the  $NVEM$  ensemble calculations, we have also used the collision rate to estimate the pressure, through Eqs. (8) and (14). These results are also shown in Table I. The agreement of these values of the pressure lends added credence to the adequacy of the present calculations in sampling phase space.

#### 4. THERMODYNAMIC LIMIT

To extrapolate our equation of state to thermodynamic limit, we recall the known  $N$  dependence for the  $NPT$  ensemble derived by Salsburg,<sup>(16)</sup>

$$Z_{NPT} = \frac{pV_{NPT}}{Nk_B T} = \sum_{i=0}^{\infty} C_i(N) p^i \quad (16)$$

<sup>4</sup> We use the Box-Muller<sup>(15)</sup> method to select velocities from the Maxwell-Boltzmann distribution. For the  $NVE$  ensemble, we rescale the resultant velocities to obtain the given energy. For the  $NVEM$  ensemble, we rescale the velocities in the center-of-mass frame of reference to obtain the given  $\hat{E}$ .



with coefficients  $C_i(N)$  which are exactly linear in  $1/N$  for  $i < N$ ,

$$C_i(N) = C_i^{(0)} + C_i^{(1)}/N \quad (17)$$

provided one neglects terms of exponential order in  $N$ . Moreover, the  $C_i^{(1)}$  are known in terms of the  $C_j^{(0)}$  for  $j \leq i$ , which, in turn, are known in terms of the ordinary virial (density) coefficients  $B_k$ ,  $k \leq j$ . Thus for  $N$  and  $p$  such that  $N$  terms of Eq. (16) are adequate to represent the equation of state, we write

$$\begin{aligned} Z_{NPT} &= Z^{(0)} + Z_{NPT}^{(1)}/N \\ Z^{(0)} &= \sum_{i=0}^{\infty} C_i^{(0)} p^i \\ Z_{NPT}^{(1)} &= \sum_{i=0}^{\infty} C_i^{(1)} p^i \end{aligned} \quad (18)$$

in which  $Z^{(0)}$  is the compressibility factor in the thermodynamic limit.

To obtain the dependence of the  $NVT$  ensemble pressure on  $N$  from the  $NPT$  ensemble result, we recall the well-known relationship,<sup>(11)</sup>

$$\beta p_{NVT}(V) = \beta p + \frac{\partial}{\partial V} P_{NPT}(V) \quad (19)$$

where  $P_{NPT}(V)$  is the distribution function for the (fluctuating) volume which for hard spheres is

$$\begin{aligned} P_{NPT}(V) &= \frac{Q_N(V) e^{-\beta p V}}{\Delta_N(\beta p)} \\ Q_N(V) &= \int_V d\mathbf{r}^N B_N(\mathbf{r}^N) \\ \Delta_N(\beta p) &= \int_0^{\infty} dV e^{-\beta p V} Q_N(V) \end{aligned} \quad (20)$$

in which  $B_N(\mathbf{r}^N)$  is the overlap function (equal to 1 unless  $|\mathbf{r}_{i2}| < \sigma$  for some  $i, j$  pair, in which case it vanishes). At the maximum  $V_{NPT}^{(m)}$  of the distribution function, then, we see that Eq. (19) reduces to

$$p_{NVT}[V_{NPT}^{(m)}] = p \quad (21)$$

Assuming that  $P_{NPT}(V)$  is unimodal, we show in the Appendix [see also Eq. (8.8) of the first paper of Ref. 11] that the transformation between the two ensembles, to leading order in  $1/N$ , is

$$\varphi_{NVT}(\tau_{NPT}) = \varphi + \frac{1}{2N} \frac{d^2 \varphi_{NVT}}{d\tau^2} \left( \frac{d\varphi_{NVT}}{d\tau} \right)^{-1} + O(N^{-2}) \quad (22)$$

where  $\varphi$  is the reduced pressure,

$$\begin{aligned}\varphi &= pV_0/Nk_B T \\ \varphi_{NVT}(\tau) &= p_{NVT}(\tau)V_0/Nk_B T\end{aligned}$$

and where the derivatives on the right-hand side are to be evaluated at the  $NPT$  ensemble expectation value,  $\tau_{NPT}$ . Dividing the Salsburg relation Eq. (18) by  $\varphi$ , we obtain

$$\tau_{NPT}(\varphi) = \tau^{(0)}(\varphi) + \tau_{NPT}^{(1)}(\varphi)/N \quad (23)$$

where  $\tau^{(0)}(\varphi)$  is the infinite-system reduced volume as a function of reduced pressure. Substituting Eq. (23) into Eq. (22), we obtain

$$Z_{NVT}(\tau) = Z^{(0)} + Z_{NVT}^{(1)}(\tau)/N + O(N^{-2}) \quad (24)$$

in which

$$Z_{NVT}^{(1)}(\tau) = -\tau\tau_{NPT}^{(1)}[\varphi^{(0)}(\tau)] \frac{d\varphi_{NVT}}{d\tau} + \frac{\tau}{2} \frac{d^2\varphi_{NVT}}{d\tau^2} \left( \frac{d\varphi_{NVT}}{d\tau} \right)^{-1} \quad (25)$$

In Eqs. (24) and (25), we have written  $\tau$  in place of  $\tau^{(0)}$  and the argument  $\varphi^{(0)}(\tau)$  of  $\tau_{NPT}^{(1)}$  is again obtained from the infinite-system equation of state. The derivatives are now evaluated at  $\tau$ .

To obtain the thermodynamic limit  $Z^{(0)}$  from  $Z_{NVT}$ , as reported in Section 3, we obtain  $Z^{(1)}$  from Eq. (25), using for  $\varphi_{NVT}$  (on the right) one of the familiar Padé approximants to the density series,

$$\begin{aligned}Z_{p/q}^{(0)} &= 1 + \frac{xP_p(x)}{Q_q(x)} \\ P_p(x) &= 1 + \sum_{i=1}^p a_i^{[p/q]} x^i \\ Q_q(x) &= 1 + \sum_{i=1}^q b_i^{[p/q]} x^i \\ x &= \frac{\pi(2\sqrt{2})}{3\tau}\end{aligned} \quad (26)$$

in which we follow the usual practice<sup>(17)</sup> of designating by  $[p/q]$  an approximant which has degrees  $p$  and  $q$  for the numerator and denominator, respectively. The  $\tau^{(1)}$  contribution can also be written as a Padé approximant (with  $x$  as argument) by substituting the virial series for the pressure into the pressure series, Eq. (16), and rearranging terms, yielding

the Padé approximant,

$$\begin{aligned} \varphi\tau_{p/q}^{(1)} - 1 &= \frac{xP_p^{(1)}(x)}{Q_q^{(1)}(x)} \\ P_p^{(1)}(x) &= 1 + \sum_{i=1}^p \alpha_i^{[p/q]} x^i \\ Q_q^{(1)}(x) &= 1 + \sum_{i=1}^q \beta_i^{[p/q]} x^i \end{aligned} \tag{27}$$

To evaluate the theoretical equation of state, Eq. (24), we use the [2/2] approximant of Kratky<sup>(8)</sup> [also called the Padé (3 × 3) or P(3, 3)] for Z<sup>(0)</sup>. We form the  $\tau_{2/2}^{(1)}$  approximant, based on the same virial coefficients  $B_1 - B_6$  and the  $C_i^{(1)}(N)$  of Salsburg,<sup>(16)</sup> to get the  $\alpha_i^{[2/2]}$  and  $\beta_i^{[2/2]}$ . From these we compute the theoretical equation of state (24) which we compare with our MCMD results in Figs. 1–6 for reduced volumes,  $\tau = 10, 5, 4, 3, 2,$  and 1.6 for which at least two different system sizes were investigated. We note that for the lowest densities, Figs. 1–3, the agreement appears quite

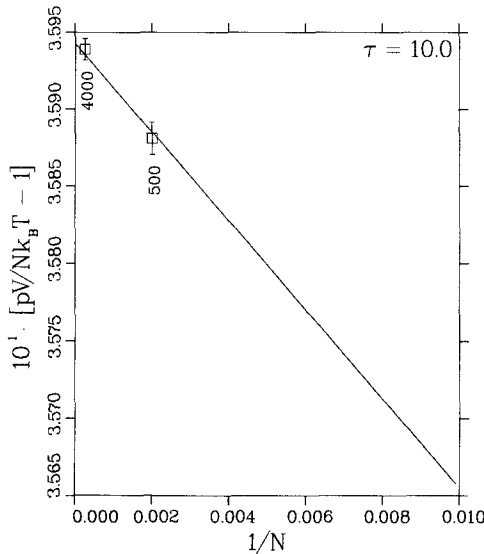


Fig. 1. The equation of state of the hard-sphere fluid at a volume  $V = 10V_0$  as a function of system size. The solid line is the theoretical Eq. (24), based on the Kratky [2/2] Padé approximant. The dashed line is based on the optimal [3/2] approximant, but is indistinguishable from the solid line except at higher density.

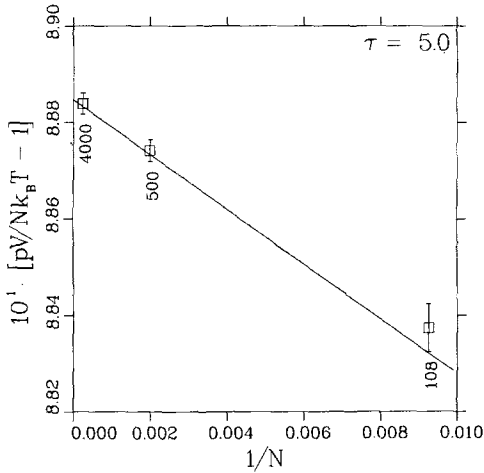


Fig. 2. Same as Fig. 1, for  $V = 5V_0$ .

satisfactory. At  $\tau = 3$ , Fig. 4, there appears to be a marginally significant deviation from the theory for the very accurate  $N = 4000$  point. This difference is amplified at  $\tau = 2$  (Fig. 5) and  $\tau = 1.6$  (Fig. 6). Moreover, for  $\tau = 1.6$ , one can see that the three points differ significantly from any straight line. It would appear that either the  $N^{-2}$  term in Eq. (24) becomes important here or that the exponential terms in  $N$  contribute appreciably to

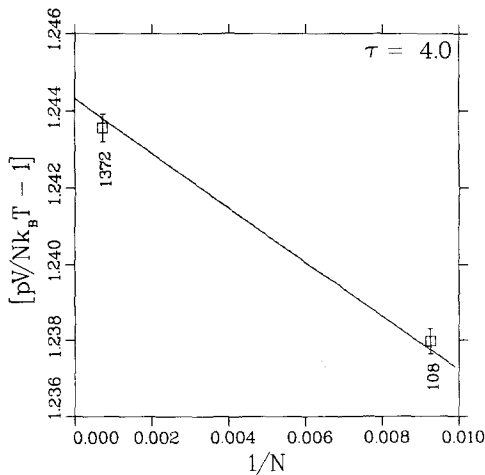


Fig. 3. Same as Fig. 1, for  $V = 4V_0$ .

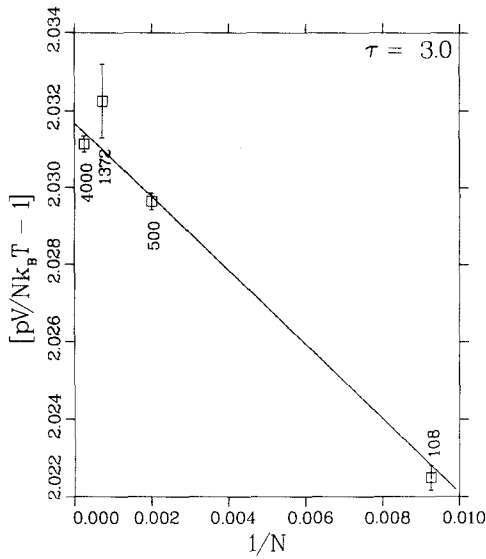


Fig. 4. Same as Fig. 1, for  $V = 3V_0$ .

the  $NPT$  ensemble pressure. In any case, because the MCMD and the theoretical  $1/N$  slopes seem to be at least in qualitative agreement for large  $N$  and for all densities, we can crudely extrapolate to the infinite system by simply subtracting  $Z^{(1)}/N$  from the largest system results in Table I.

A better procedure is to fit the MCMD data to the theoretical Eq. (24) by rewriting the latter in terms of Padé approximants in which the sixth

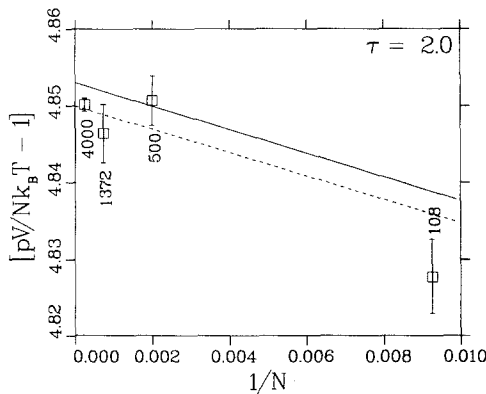


Fig. 5. Same as Fig. 1, for  $V = 2V_0$ .

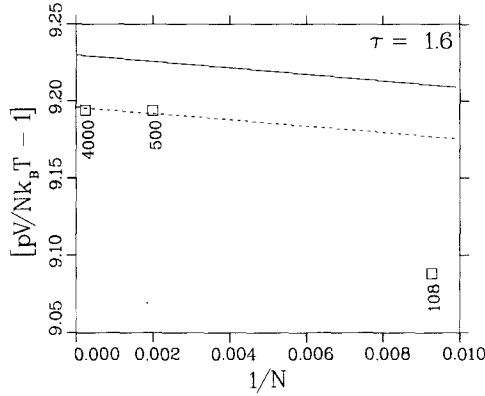


Fig. 6. Same as Fig. 1, for  $V = 1.6V_0$ .

and seventh virial coefficients appear as parameters. The known Monte Carlo estimates for  $B_6$  and  $B_7$  contain sizeable uncertainties,<sup>(8)</sup>

$$\begin{aligned}
 B_6/B_2^5 &= 0.0389 \pm E_6 \\
 E_6 &= 0.004 \\
 B_7/B_2^6 &= 0.0137 \pm E_7 \\
 E_7 &= 0.006
 \end{aligned}
 \tag{28}$$

If we write

$$\begin{aligned}
 B_6/B_2^5 &= 0.0389 + f_6 E_6 \\
 B_7/B_2^6 &= 0.0137 + f_7 E_7
 \end{aligned}
 \tag{29}$$

then we define the parametric form of Eq. (24),

$$Z_{p/q}(\tau, N; f_6, f_7) = Z_{p/q}^{(0)}(\tau; t_6, f_7) + Z_{p/q}^{(1)}(\tau; f_6, f_7)/N \tag{30}$$

in which the coefficients  $a_i^{[p/q]}$  and  $b_i^{[p/q]}$  of  $Z_{p/q}^{(0)}$ , Eq. (26), and the coefficients  $\alpha_i^{[p/q]}$  and  $\beta_i^{[p/q]}$  of  $\tau_{p/q}^{(1)}$ , Eq. (27), are based on the known values of  $B_1$  through  $B_4$ , Kratky's<sup>(8)</sup> precise Monte Carlo estimate for  $B_5$  ( $0.110252B_2^4$ ), and the values of  $B_6$  and  $B_7$  from Eq. (29). If we denote the MCMD values by  $Z(\tau, N)$  with standard deviations  $s(\tau, N)$  as given in Table I, then the quantity,

$$\begin{aligned}
 \chi_{p/q}^2(f_6, f_7) &= \sum_{\tau} \sum_N \chi_{p/q}^2(\tau, N; f_6, f_7) \\
 \chi_{p/q}^2(\tau, N; f_6, f_7) &= \left[ \frac{Z(\tau, N) - Z_{p/q}(\tau, N; f_6, f_7)}{s(\tau, N)} \right]^2
 \end{aligned}
 \tag{31}$$

in which the  $\tau$  and  $N$  sums run over the available entries, Table I, represents the goodness of fit for given  $f_6$  and  $f_7$ . Thus,  $\chi_{p/q}^2(f_6, f_7)$  can be minimized with respect to its parameters in a nonlinear least-squares procedure. We label the resultant values of the parameters by  $f_6^*$  and  $f_7^*$ . Under the hypothesis that the MCMD data are samples from a normal distribution with mean given by Eq. (30), the statistic  $\chi_{p/q}^2(f_6^*, f_7^*)$  is expected to have the  $\chi^2$  distribution.

In the first instance, we attempted to fit only  $f_6$  by using the [2/2] approximant which is independent of  $B_7$ . The optimum fit, however, showed a large, statistically significant value for  $\chi^2$ . Instead, then, we use both the [3/2] and the [2/3] approximants, performing the nonlinear least-squares for each choice. These approximants depend on the virial coefficients through  $B_7$  and lie near the  $p = q$  "diagonal" for which the Padé approximants are believed to be best in improving the convergence of the virial series.

In performing the least squares, we do not include the  $N = 108, \tau = 1.6$  point inasmuch as it appears from Fig. 6 to lie outside the range of validity of the  $1/N$  "correction." The point at  $N = 108, \tau = 2$  is somewhat more problematic; see Fig. 5. As a result we perform the least-squares analysis both including this point (yielding 19 degrees of freedom,  $\nu$ , for the optimum fit) and excluding it ( $\nu = 18$ ). The results of this analysis for both the [3/2] and the [2/3] cases are given in Table II. The column labeled  $P(\chi^2, \nu)$  is the cumulative distribution at the observed value of the  $\chi^2$  at the optimum fit.

As an optimal choice, we select the [3/2] approximant with  $f_6^* = 0.2394$  and  $f_7^* = 1.0556$ . These values yield estimates for  $B_6$  and  $B_7$  which are in adequate agreement with the Monte Carlo estimates, Eq. (29). The coefficients of the optimal [3/2] approximant are given in Table III. The contributions  $\chi_{3/2}^2(\tau, N; f_6^*, f_7^*)$ , Eq. (31), to  $\chi^2$  from each individual MCMD datum are tabulated in Table I in the column labeled  $\chi^2$ . It is notable that the principal contributions to the overall  $\chi^2$  statistic arise from the  $\tau = 25$  and  $\tau = 1.6$  data, along with the  $N = 4000, \tau = 3$  point. While none of these deviations is as large as two standard deviations, there is

**Table II. Least-Square Fit of Padé Approximants to MCMD Equation of State**

$[p/q]$	$f_6^*$	$f_7^*$	$\nu$	$\chi^2$	$P(\chi^2, \nu)$
2/3	0.2730	-1.0670	18	17.8	0.5
	0.2510	-1.0737	19	20.7	0.6
3/2	0.2394	-1.0556	18	17.4	0.5
	0.2227	-1.0622	19	20.2	0.6

**Table III. Coefficients for the Optimal [3/2] Padé Approximant for the Hard-Sphere Equation of State**

$i$	1	2	3
$a_i^{[3/2]}$	0.0556782	0.01394451	-0.00133996
$b_i^{[3/2]}$	-0.056943218	0.08289011	—

perhaps some suggestion that the highest-density data signal the outset of systematic deviations from the [3/2] representation. Finally, the optimal  $N$ -dependent representation,

$$Z^*(\tau, N) = Z_0^*(\tau) + Z_1^*(\tau)/N \quad (32)$$

$$Z_i^*(\tau) = Z_{3/2}^{(i)}(\tau; 0.2394, -1.0556)$$

is plotted as a dashed line in Figs. 1–6.

The uncertainties of our estimates of  $B_6$  and  $B_7$  are difficult to assess accurately. While one could readily obtain the ellipse in the  $f_6, f_7$  plane on which  $\chi^2$  attains the 95 percentile level, it seems virtually certain that systematic deviations in the [3/2] (or [2/3]) Padé approximant from the true equation of state are more important than any statistical uncertainty in our data. A better estimate of the uncertainty in  $B_6$  and  $B_7$  is provided by the variation among the values given in Table II.

We can also compute the virial coefficients  $B_n$ ,  $n > 7$ , from our optimal approximant. We obtain for  $B_n/B_2^{n-1}$  0.00421, 0.00131, and 0.00040 for  $n = 8, 9$ , and 10, respectively. These values are close to a number of the approximate values given by Kratky.<sup>(8)</sup> In particular, they differ from the Carnahan–Starling values only in the last digit.

It is perhaps worthwhile to take note of the attempts<sup>(9,10,18)</sup> to base approximants on the supposition that the virial series should diverge at some high density, for example, the close-packed volume  $\tau = 1$  or the random-dense-packed volume  $\tau \approx 1.16$ . While the Kratky [2/2] approximant has a pair of singularities at densities above the close-packed lattice density, it is also true that a number of different approximants, based on these same Ree–Hoover–Kratky virial coefficients, including the [2/3] and the [3/2] approximants, in fact have real singularities with  $\tau$  near the random close packing.<sup>(19)</sup> Nonetheless, when we recompute these approximants using our fitted values of  $B_6$  and  $B_7$  (based on fitting either the [3/2] or the [2/3] approximant), we find that the [3/2] and the [2/3] approximants, in addition to the [2/2], now have singularities with  $|\tau| < 1$  and well removed from the random close packed point. It seems, therefore, that the virial coefficients are not known with sufficient precision to locate the singularities of the virial series.



## 5. COMPARISON WITH ANALYTIC EQUATIONS

A large number of theoretical and phenomenological equations have been proposed for the hard-sphere equation of state. We have compared our infinite-system representation  $Z_0^*(\tau)$  with many of these, including the Carnahan–Starling<sup>(20)</sup> equation, the Percus–Yevick<sup>(21)</sup> “compressibility” equation, the Ree–Hoover<sup>(7)</sup> and the Kratky<sup>(8)</sup> [2/2] Padé approximants, the equations proposed by Woodcock,<sup>(22)</sup> by Andrews,<sup>(23)</sup> and by Speedy,<sup>(24)</sup> the empirical equation of Devore and Schneider,<sup>(18)</sup> and the equation recently proposed by Shinomoto.<sup>(25)</sup> We also compare our results with the Levin and Tova approximants obtained by Baram and Luban.<sup>(9)</sup> These comparisons are shown in Fig. 7a, in which we plot the difference,

$$\Delta Z(\tau) = Z(\tau) - Z_0^*(\tau) \quad (33)$$

over the entire fluid range, with  $Z(\tau)$  given by one of these analytic representations. Also shown on the figure are the MCMD data in the form of  $Z(\tau, 4000) - Z_1^*(\tau)/N$ , i.e., the 4000-particle observed equation of state, extrapolated to the thermodynamic limit via the optimal Padé approximant.

None of these relations agree with the MCMD results except at low density. The Devore–Schneider equation, which does not yield correct values for the virial coefficients, disagrees with the data even at low density. The Levin and Tova approximants shown are those of degree 6; those of degree 5 and 7 fit the data similarly. It is interesting that the Kratky [2/2] Padé approximant and the equation of Speedy appear to be the most accurate among these representations.

In Fig. 7b we show a similar plot, but displaying a number of approximants which are based on our adjusted values of  $B_6$  and  $B_7$ , in addition to the Speedy and Kratky curves. The Tova approximant of degree 6 obtained from our modified virial coefficients is labeled Tova(\*). The modified [2/2] Padé approximant is also shown, labeled [2/2]\*. The modified Levin approximant of degree 6 is labeled Levin(\*). It is notable that all three of these representations appear to suffer as approximations to the data compared to those based on the unmodified Ree–Hoover–Kratky sixth virial coefficient. However, the [2/3] Padé approximant based on our optimal values, viz.,  $f_6^* = 0.2394$ ,  $f_7^* = -1.0556$ , (and not itself fitted to the data) is labeled [2/3]\* in Fig. 7b. It is seen to fit the MCMD data more accurately than any other representation not fit to the data, i.e., other than our optimal [3/2] or [2/3] representations. This agreement would appear to indicate that the current estimates for the sixth and seventh virial coefficients are, in fact, more accurate than the Ree–Hoover–Kratky values; a proof that this is so is not possible from such an indirect method of calculation.

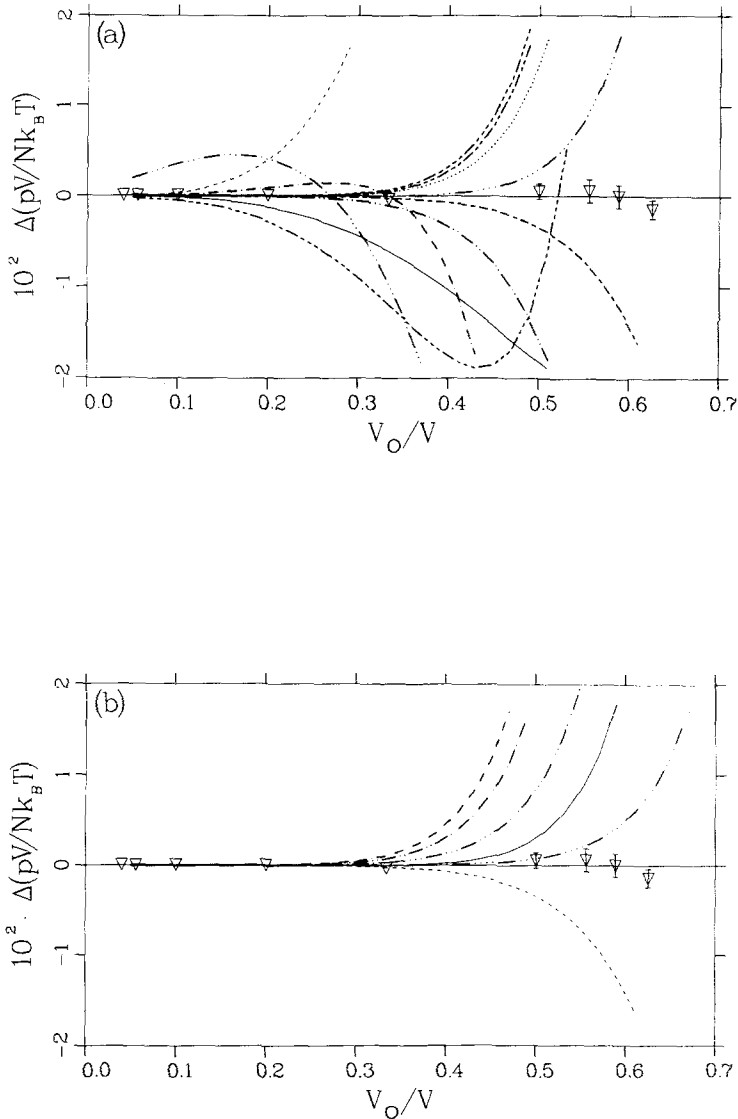


Fig. 7. The difference, Eq. (33), between the optimal [3/2] Padé approximant and various analytic equations. The points are  $N = 4000$  MCMD results, extrapolated to the thermodynamic limit. In (a): Carnahan–Starling (—), Percus–Yevick compressibility (---), Shinomoto (----), Ree–Hoover (-----), Devore–Schneider (-----), Kratky (-----), Speedy (---), Woodcock (----), Andrews (-----), Baram–Luban (Levin) (-----) and (Tova) (···). In (b): Kratky (—), Speedy (---), Tova\* (---), Levin\* (-----), [2/2]\* (-----), and [2/3]\* (-----).

It should perhaps be pointed out that the Levin and Tova approximants could be fitted to our data in the same manner as the Padé approximants, by adjusting the values of  $B_6$  and  $B_7$ . It would be interesting to see whether an equally accurate representation would be obtained and the adjusted virial coefficients would agree with the current values.

## ACKNOWLEDGMENTS

The authors wish to express their appreciation to J. L. Lebowitz for urging the publication of these results. We are also grateful to George A. Baker, Jr. for the use of his computer program in the evaluation of the many Padé approximants required, and to K. W. Kratky.

## APPENDIX

In this appendix we derive the relation between the  $NPT$  and  $NVT$  ensemble equation of state to the leading order in  $1/N$ . We begin with the exact relation Eq. (21) and compute the difference

$$\tau_{NPT} - \tau_m = \Delta_N^{-1} \int_0^\infty d\tau (\tau - \tau_m) f(\tau) \quad (\text{A1})$$

where  $\tau_m \equiv V_{NPT}^{(m)}/V_0$  and from Eq. (20) on conversion to reduced variables,

$$f(\tau) = e^{-N\varphi\tau} Q_N(\tau) \equiv e^{-Nh(\tau)} = P_{NPT}(V) \quad (\text{A2})$$

$$\Delta_N = \int_0^\infty d\tau f(\tau) \quad (\text{A3})$$

$$h(\tau) = \varphi\tau - N^{-1} \ln Q_N(\tau) \quad (\text{A4})$$

Because  $-k_B T \ln Q_N(\tau)$  is the free energy in the  $NVT$  ensemble, we see that  $h(\tau)$  is finite in the limit of large  $N$ , whence  $f(\tau)$  is expected to be peaked near its maximum. Thus we expand  $h(\tau)$  in a power series about  $\tau_m$ , using

$$\varphi_{NVT}(\tau) = \frac{1}{N} \frac{dQ_N(\tau)}{d\tau}$$

and integrate Eqs. (A1) and (A3) term by term to obtain

$$\tau_{NPT} - \tau_m = \frac{1}{2N} \frac{d^2\varphi_{NVT}(\tau_m)}{d\tau_m^2} \left[ \frac{d\varphi_{NVT}(\tau_m)}{d\tau_m} \right]^{-1} + O(N^{-2}) \quad (\text{A5})$$

Substituting  $\tau_m$  from Eq. (A5) into Eq. (21), we get

$$\varphi_{NVT}(\tau_{NPT}) = \varphi + \frac{1}{2N} \frac{d^2 \varphi_{NVT}(\tau_m)}{d\tau_m^2} \left[ \frac{d\varphi_{NVT}(\tau_m)}{d\tau_m} \right]^{-1} + O(N^{-2}) \quad (\text{A6})$$

Finally, we substitute for  $\tau_m$  from Eq. (A5) into the right-hand side of Eq. (A6) to obtain Eq. (22).

## REFERENCES

1. N. A. Metropolis, A. W. Rosenbluth, M. N. Rosenbluth, A. H. Teller, and E. Teller, *J. Chem. Phys.* **21**:1087 (1953).
2. W. W. Wood and J. D. Jacobson, *J. Chem. Phys.* **27**:1207 (1957); **12**:292 (1975).
3. B. J. Alder and T. E. Wainwright, *J. Chem. Phys.* **27**:1208 (1957).
4. W. W. Wood, Monte Carlo studies of simple liquid models, in *Physics of Simple Liquids*, H. N. V. Temperley, J. S. Rowlinson, and G. S. Rushbrooke, eds. (North-Holland, Amsterdam, 1968), Chap. 5.
5. J. A. Barker and D. Henderson, *Molec. Phys.* **21**:187 (1971).
6. J. A. Barker and D. Henderson, *Rev. Mod. Phys.* **48**:587 (1976).
7. F. H. Ree and W. G. Hoover, *J. Chem. Phys.* **40**:939 (1964); **46**:4181 (1967).
8. K. W. Kratky, *Physica* **85A**:607 (1976); **87A**:584 (1977).
9. A. Baram and M. Luban, *J. Phys. C.: Solid State Phys.* **12**:L659 (1979).
10. C. A. Angell, J. H. R. Clarke, and L. V. Woodcock, in *Advances in Chemical Physics*, Vol. 48, S. A. Rice and E. Prigogine, eds. (Wiley, New York, 1981), p. 397.
11. W. W. Wood, *J. Chem. Phys.* **48**:415 (1968); **52**:729 (1970).
12. W. W. Wood, *Acta Phys. Austriaca*, **Suppl. X**:451 (1973).
13. J. J. Erpenbeck and W. W. Wood, *J. Stat. Phys.* **24**:455 (1981).
14. J. J. Erpenbeck and W. W. Wood, Molecular Dynamics Techniques for Hard Core Systems, in *Modern Theoretical Chemistry, Vol. 6, Statistical Mechanics, Part B: Time Dependent Process*, B. J. Berne, ed. (Plenum Press, New York, 1977).
15. B. Jansson, *Random Number Generators* (Pettersons, Stockholm, 1966).
16. Z. W. Salsburg, *J. Chem. Phys.* **44**:3090 (1966); **45**:2719 (1966).
17. G. A. Baker, *Essentials of Padé Approximants* (Academic Press, New York, 1975).
18. J. A. Devore and E. Schneider, *J. Chem. Phys.* **77**:1067 (1982).
19. V. C. Aguilera-Navarro, M. Fortes, M. de Llano, and A. Plastino, *J. Chem. Phys.* **76**:749 (1982); G. A. Baker, Jr., G. Gutierrez, and M. de Llano, *Ann. Phys. (N.Y.)* (in press).
20. N. F. Carnahan and K. E. Starling, *J. Chem. Phys.* **51**:635 (1969).
21. J. K. Percus and G. J. Yevick, *Phys. Rev.* **110**:1 (1958); M. S. Wertheim, *J. Math. Phys.* **5**:643 (1964); E. Thiele, *J. Chem. Phys.* **39**:474 (1963).
22. L. V. Woodcock, *J. Chem. Soc. Faraday Trans. 2* **72**:731 (1976).
23. F. C. Andrews, *J. Chem. Phys.* **64**:1941 (1976).
24. R. J. Speedy, *J. Chem. Soc. Faraday Trans. 2* **75**:1643 (1979).
25. S. Shinomoto, *J. Stat. Phys.* **32**:105 (1983).